

# Three-Dimensional Optical Coherence Tomography Imaging For Glaucoma Associated With Boston Keratoprosthesis Type I and II

Ziad Khoueir, MD,\*†‡, Firas Jassim, PhD,\*†, Boy Braaf, PhD,\*§  
 Linda Yi-Chieh Poon, MD,\*†||, Edem Tsikata, PhD,\*†  
 James Chodosh, MD, MPH,\*†, Claes H. Dohlman, MD, PhD,\*†  
 Benjamin J. Vakoc, PhD,\*§, Brett E. Bouma, PhD,\*§  
 Johannes F. de Boer, PhD,¶# and Teresa C. Chen, MD\*†

**Precis:** Three-dimensional (3D) spectral domain optical coherence tomography (OCT) volume scans of the optic nerve head (ONH) and the peripapillary area are useful in the management of glaucoma in patients with a type I or II Boston Keratoprosthesis (KPro).

**Purpose:** The purpose of this study was to report the use of spectral domain OCT in the management of glaucoma in patients with a type I or II Boston KPro.

**Materials and Methods:** This study is an observational case series. Four consecutive patients with KPro implants were referred for glaucoma evaluation. A comprehensive eye examination was

performed which included disc photography, visual field testing, and high-density spectral domain OCT volume scans of the ONH and the peripapillary area. 2D and 3D parameters were calculated using custom-designed segmentation algorithms developed for glaucoma management.

**Results:** Spectral domain OCT parameters provided useful information in the diagnosis and management of 4 KPro patients. OCT parameters which can be used in KPro patients included 2D retinal nerve fiber layer (RNFL) thickness, 3D peripapillary RNFL volume, 3D peripapillary retinal thickness and volume, 3D cup volume, and 3D neuroretinal rim thickness and volume. In 3 of 4 cases where the traditional 2D RNFL thickness scan was limited by artifacts, 3D spectral domain OCT volume scans provided useful quantitative objective measurements of the ONH and peripapillary region. Therefore, 3D parameters derived from high-density volume scans as well as radial scans of the ONH can be used to overcome the limitations and artifacts associated with 2D RNFL thickness scans.

**Conclusions:** Spectral domain OCT volume scans offer the possibility to enhance the evaluation of KPro patients with glaucoma by using both 2D and 3D diagnostic parameters that are easily obtained in a clinic setting.

**Key Words:** glaucoma, keratoprosthesis, spectral domain optical coherence tomography, retinal nerve fiber layer, diagnosis

(*J Glaucoma* 2019;28:718–726)

Received for publication January 21, 2019; accepted May 5, 2019.  
 From the \*Harvard Medical School; †Department of Ophthalmology, Massachusetts Eye and Ear; §Wellman Center for Photomedicine, Massachusetts General Hospital, Boston, MA; ‡Beirut Eye & ENT Specialist Hospital, Saint-Joseph University Medical School, Beirut, Lebanon; ||Department of Ophthalmology, Kaohsiung Chang Gung Memorial Hospital, Chang Gung University College of Medicine, Kaohsiung, Taiwan; ¶LaserLaB, Department of Physics and Astronomy, Vrije Universiteit Amsterdam; and #Department of Ophthalmology, Vrije Universiteit Medical Center, Amsterdam, The Netherlands.

T.C.C. has received funding from Fidelity Charitable Fund (Harvard University), the American Glaucoma Society Mid-Career Award, the Massachusetts Lions Research Eye Fund, the Harvard Catalyst National Institutes of Health UL1 RR025758, and the Department of Defense Small Business Innovation Research DHP15-016. B.B., B.J.V., and B.E.B. received funding from the Center for Biomedical OCT Research and Translation through Grant Number P41EB015903, awarded by the National Institute of Biomedical Imaging and Bioengineering of the National Institutes of Health.

**Disclosure:** J.C., C.H.D., and T.C.C. work at the Massachusetts Eye and Ear, a nonprofit hospital and distributor of the Boston Keratoprosthesis. J.F.d.B. has the following financial disclosures: Center for Biomedical Optical Coherence Tomography Research and Translation Scientific Advisory Board Chair (Harvard Medical School), licenses to NIDEK Inc, Terumo Corporation, Ninepoint Medical, and Heidelberg Engineering. B.J.V. licenses to Terumo Corporation (Tokyo, Japan) and Ninepoint Medical (Bedford, Massachusetts). B.E.B. licenses to NIDEK Inc. (Fremont, CA), Terumo Corporation, Ninepoint Medical, Heidelberg Engineering. The remaining authors declare no conflict of interest.

**Reprints:** Teresa C. Chen, MD, Department of Ophthalmology, Massachusetts Eye and Ear, Glaucoma Service, 243 Charles Street, Boston, MA 02114 (e-mail: teresa\_chen@meei.harvard.edu).

Copyright © 2019 The Author(s). Published by Wolters Kluwer Health, Inc. This is an open-access article distributed under the terms of the Creative Commons Attribution-Non Commercial-No Derivatives License 4.0 (CCBY-NC-ND), where it is permissible to download and share the work provided it is properly cited. The work cannot be changed in any way or used commercially without permission from the journal.

DOI: 10.1097/IJG.0000000000001280

**B**oston Keratoprosthesis (KPro) surgery is indicated in patients who have failed repeated penetrating keratoplasty procedures or who have a high risk for penetrating keratoplasty failure. Although KPro surgery can offer a useful vision in patients with no other alternatives, this vision can be limited by glaucoma, which is one of the most common complications of KPro surgery.<sup>1,2</sup> Several papers have reported that the incidence of glaucoma before KPro implantation is between 36% and 76%,<sup>3–11</sup> and KPro surgery has been associated with progression of preexisting glaucoma. Furthermore, new-onset glaucoma can occur as a complication of KPro surgery in 2% to 28% of the patients<sup>3,7–9,11–13</sup> and can progress quickly.<sup>1</sup>

The diagnosis and management of glaucoma in KPro patients is difficult because clinical testing is limited and difficult to obtain. For example, it is not possible to measure the intraocular pressure (IOP) with standard tonometry techniques due to the rigidity of the KPro device.<sup>14</sup> Because of the small KPro optic and because of the potential for retroprosthetic membranes, disc photography is challenging,

and visual field (VF) testing is unreliable in over half of patients.<sup>1</sup> Also, although optical coherence tomography (OCT) posterior segment imaging is a mainstay of glaucoma management,<sup>15–18</sup> published studies of KPro and OCT have largely been limited to anterior segment OCT.<sup>19,20</sup> Because of the paucity of posterior segment OCT articles in the KPro glaucoma literature, this paper seeks to evaluate the utility of posterior segment OCT for the evaluation of KPro glaucoma patients.

This paper focuses on the OCT examination of the optic nerve and the peripapillary retina in KPro patients. Imaging holds the potential for the early detection of glaucoma disease progression,<sup>21</sup> because structural changes of the optic nerve head (ONH) and the retinal nerve fiber layer (RNFL) can occur before VF loss. Imaging also affords more objectivity in the glaucoma examination. For example, clinical determination of the ONH is highly subjective with significant interexaminer variability since studies have demonstrated that 4% to 19% of the cup to disc ratio estimates made by 2 different glaucoma specialists differed by  $\geq 0.2$ .<sup>22,23</sup> Lastly, Kumar et al<sup>24</sup> reported good quality OCT images of the optic nerve through the 3.5 to 4.0 mm optic of a similar device, the osteo-odonto-keratoprosthesis. The quality of imaging through the smaller 3.0 mm optic of the KPro has never been reported.<sup>14</sup> The purpose of this report is to show that structural assessment of the ONH and RNFL can be performed in KPro patients and that this tool should be integrated into their management.

## MATERIALS AND METHODS

### Patient Recruitment

All 4 KPro patients were recruited at the Massachusetts Eye and Ear between June 2015 and October 2015. The research protocol was approved by the Massachusetts Eye and Ear Institutional Review Board. All methods adhered to the tenets of the Declaration of Helsinki for research involving human subjects, and the study was conducted in accordance with Health Insurance Portability and Accountability Act regulations. Informed consent was obtained from all subjects. All study subjects underwent a complete eye examination by a glaucoma specialist (T.C. C.), and this included history, visual acuity testing, slit-lamp biomicroscopy, dilated ophthalmoscopy, stereo disc photography (Visucam Pro NM; Carl Zeiss Meditec Inc.), VF testing (Swedish Interactive Threshold Algorithm 24-2 test of the Humphrey visual field analyzer 750i; Carl Zeiss Meditec Inc.), and OCT imaging (HRA/Spectralis software version 5.4.8.0; Heidelberg Engineering GmbH, Heidelberg, Germany).

### Definition of Glaucoma

Patients were deemed to have preexisting glaucoma if before KPro surgery there was a history of glaucoma, chronic glaucoma medication use, or prior glaucoma surgery, which includes glaucoma drainage device implantation, trabeculectomy, or cyclophotocoagulation. A new postoperative diagnosis of glaucoma was defined as having advanced optic nerve cupping (cup to disc ratio  $\geq 0.7$ ), needing chronic glaucoma medications, and/or requiring glaucoma surgery.

### Imaging Protocol

All patients in our study were imaged through the KPro optic with the Heidelberg Spectralis SD-OCT

machine. Four imaging protocols were used in this study: (1) a circle scan for 2-dimensional (2D) RNFL thickness (Fig. 1A) (2) a 24-line radial scan over the optic nerve for Bruch's membrane opening-minimum rim width assessment (BMO-MRW) (Fig. 1B) (3) a vertical line scan through the optic nerve for cup to disc ratio calculation (Fig. 1C), and (4) a 20×20 degrees volume scan of the optic nerve consisting of 193 raster B-scans for peripapillary RNFL volume, peripapillary retinal volume, minimum distance band (MDB) neuroretinal rim thickness, and neuroretinal rim volume calculations (Fig. 1D).

### Software Used

Two-dimensional RNFL thickness was obtained from the peripapillary circle scans using data analysis performed with the Heidelberg Eye Explorer (software version 1.9.10.0; Heidelberg Engineering GmbH) (Fig. 1A).

BMO-MRW was obtained from the radial scans with analysis also performed by the Heidelberg Eye Explorer (software version 1.9.10.0; Heidelberg Engineering GmbH) (Fig. 1B). It is a diagnostic rim parameter measuring the thickness of the neuroretinal rim tissue between the edges of the Bruch's membrane (BM) and the closest point on the retinal surface.<sup>25</sup>

As a 150- $\mu$ m reference plane above the retinal pigment epithelium (RPE) is classically used to determine optic nerve parameters,<sup>26</sup> a C++ code was used to calculate the vertical cup to disc ratio along this standard reference plane (Fig. 1C). The disc border was defined as the RPE/BM complex, and cup border was defined as the intersection of the cup surface with this reference plane.

Each 6 mm by 6 mm volume scan was processed with an algorithm written in C++ to calculate the neuroretinal rim MDB thickness (Fig. 1D). The MDB is a 3D neuroretinal rim parameter and is defined as the circular band delimited by the shortest distance between the RPE/BM complex and the internal limiting membrane or cup surface.<sup>21</sup>

Each 6 mm by 6 mm volume scan was then processed using an algorithm developed with MATLAB software version 2012a (MathWorks Inc., Natick, MA). The segmentation algorithm identified the internal limiting membrane, the posterior border of the RNFL, and the RPE using edge and intensity information (Fig. 1D). The software identified the center of the optic disc using the spatial information provided by the terminations of the RPE. To determine peripapillary RNFL volume and total retinal volume, 4 different annuli were used. Each peripapillary 3D annulus had a width of 1 mm. The smallest circumpapillary annulus (CA) 1 was defined by an inner diameter of 2.5 mm and an outer diameter of 3.5 mm, larger CA2 by diameters of 3 and 4 mm, larger CA3 by diameters of 3.5 and 4.5 mm, and largest CA4 by diameters of 4 and 5 mm. The automated interface processed the 193 images of each volume scan to calculate 3D RNFL volume and 3D retinal volume for the overall annulus, each quadrant, and 4 octants (ie, superior temporal, superior nasal, inferior temporal, and inferior nasal).

## RESULTS

### Case 1

A 65-year-old white woman was referred to our department for a glaucoma evaluation. Four years before imaging, she had surgery for a type II KPro and Ahmed glaucoma valve (New World Medical, Rancho Cucamonga,

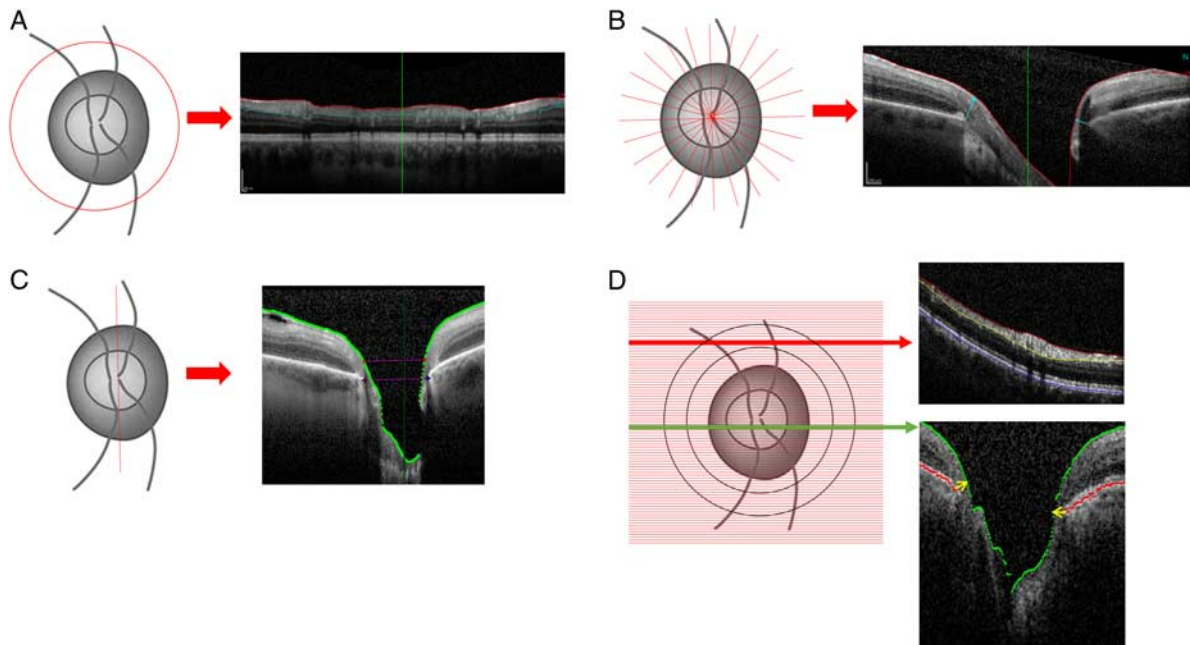


**FIGURE 1.** Simplified schematic representations of the 4 optical coherence tomography (OCT) imaging scan protocols used in this study, with a red or green arrow pointing to its associated OCT image. A, The peripapillary circle scan was used to determine 2-dimensional retinal nerve fiber layer (RNFL) thickness (software version 1.9.10.0; Heidelberg Engineering GmbH). B, Radial line scans through the optic nerve head were used to calculate Bruch’s membrane opening-minimum rim width (BMO-MRW, software version 1.9.10.0; Heidelberg Engineering GmbH). This simplified schematic only displays 12 radial line scans, but the actual commercially available software uses 24 radial line scans. The BMO-MRW measures neuroretinal rim thickness in 3-dimensional (3D) space, with the blue arrows representing the shortest distance between the Bruch’s membrane opening and the retinal surface. C, A vertical line scan going through the center of the optic nerve head was used to calculate the cup to disc ratio using the reference plane 150  $\mu\text{m}$  above the retinal pigment epithelium (RPE). D, A 6 mm by 6 mm high-density volume scan consisting of 193 B-scans was used for this study; however, this simplified schematic only displays 86 raster lines. Using customized MATLAB software (long thin red arrow), 3D peripapillary RNFL volume and 3D peripapillary retinal volume for different annuli sizes were calculated. Using C++ software (long thin green arrow), 3D neuroretinal rim thickness was calculated as the minimum distance band (yellow arrows) or the shortest distance between the RPE/Bruch’s membrane complex and the internal limiting membrane. Using a 150  $\mu\text{m}$  reference plane, 3D neuroretinal rim volume was also calculated.

CA) for her right eye due to refractory ocular cicatricial pemphigoid. Glaucoma was diagnosed before the KPro surgery, and the patient was maintained on oral acetazolamide 500 mg bid after the surgery. At the time of imaging, her best-corrected visual acuity (BCVA) was 20/40, and her IOP was estimated to be around 12 mm Hg by finger palpation. The patient had a 0.8 cup to disc ratio with thinning of the superior and inferior neuroretinal rim. This was compatible with a superior and inferior arcuate defect in her VF test with a mean deviation (MD) of  $-21.38$  dB (Fig. 2A). The global RNFL thickness value reported by the Heidelberg software was 102  $\mu\text{m}$  and was identified to be within normal limits on the OCT report. This overestimation of 2D RNFL thickness was due to a segmentation artifact of the posterior border of the RNFL despite the good signal strength of the image that was above 15 dB (Fig. 2B). The OCT cup to disc ratio calculated by the C++ code was 1.0 when using a 150  $\mu\text{m}$  reference plane (Fig. 2C). The BMO-MRW analysis showed severe neuroretinal rim thinning (Fig. 2D). All quadrants and sectors except for the temporal quadrant were coded as red or outside normal limits. The average global BMO-MRW value was 161  $\mu\text{m}$  ( $<1\%$ ) which is consistent with glaucomatous neuropathy.

**Case 2**

A 56-year-old white woman was referred to our department for glaucoma evaluation. Seven years before

imaging, she had type I KPro surgery in her left eye due to Stevens-Johnson syndrome. One year after KPro surgery, endoscopic cyclophotocoagulation was performed due to IOP elevation. After endoscopic cyclophotocoagulation, her BCVA was 20/70, and her IOP was well controlled between 10 and 15 mm Hg, with 1 topical medication (timolol maleate 0.5% bid). Her clinical examination finding of a 0.3 nasal rim with inferior neuroretinal rim thinning was consistent with a superior paracentral VF defect with an MD of  $-12.05$  dB (Fig. 3A). The average global RNFL thickness value reported by the Heidelberg software was 68  $\mu\text{m}$  and was therefore coded red or outside normal limits on the OCT report. The vertical cup to disc ratio calculated by the C++ code was 0.8 (Fig. 3B).

**Case 3**

A 41-year-old white male patient was referred to our department for glaucoma evaluation after a severe alkali burn. One year before imaging, the patient had type I KPro and Ahmed glaucoma valve surgery for his right eye. At the time of imaging, his BCVA was 20/60, and the estimated IOP was 15 mm Hg by finger palpation while on topical brimonidine tartrate 0.2% bid. The view was very poor, and he appeared to have a cup to disc ratio of 0.2 on the fundusoscopic examination (Fig. 4A). He had a superior arcuate scotoma on VF testing and an MD of  $-15.65$ . The average global RNFL thickness was 92  $\mu\text{m}$  and was therefore reported to be within normal

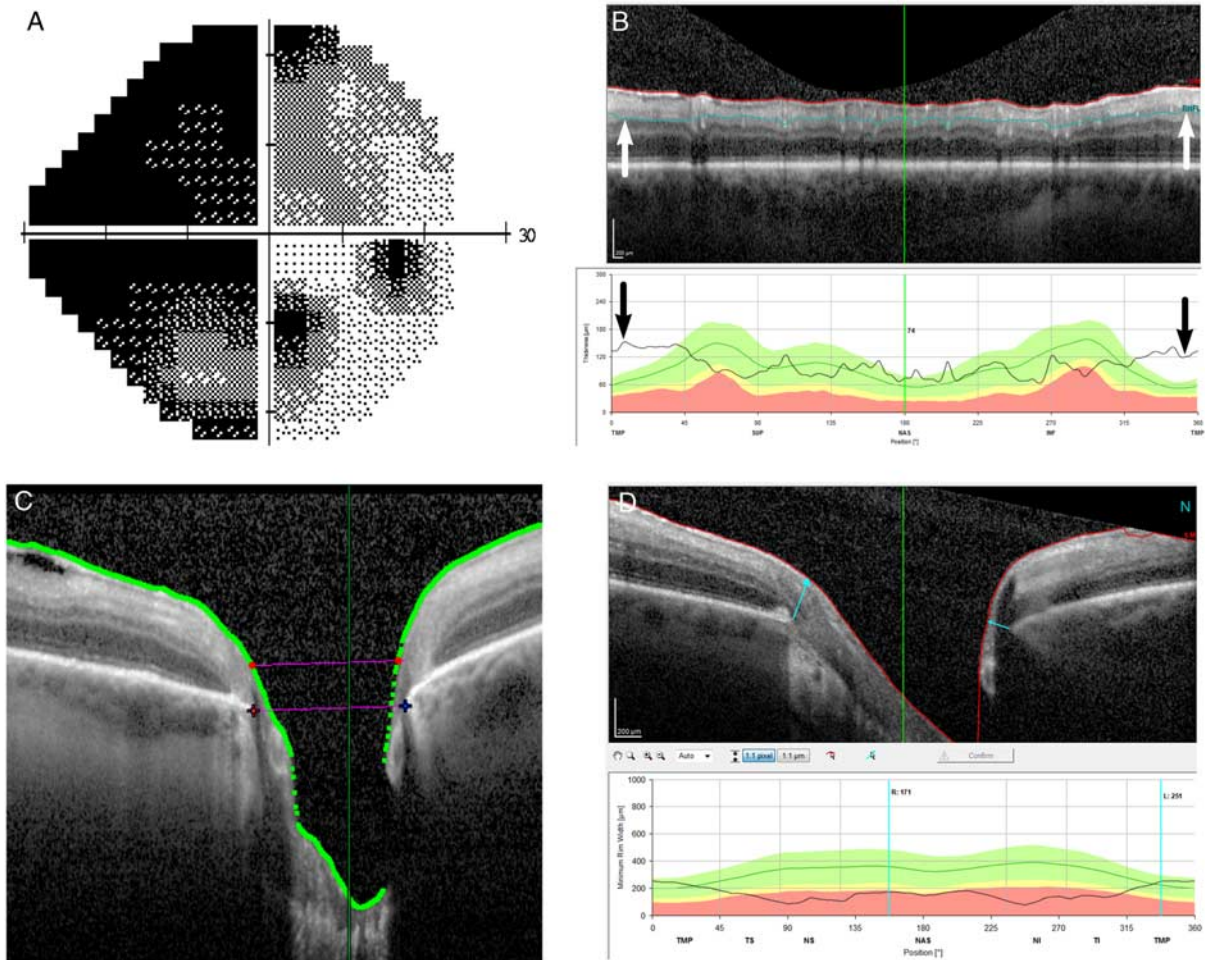


**FIGURE 2.** The clinical testing obtained in a 65-year-old white female who had a type II Boston Keratoprosthesis in her right eye for ocular cicatricial pemphigoid. A, Humphrey visual field testing showed a dense superior and inferior arcuate scotoma. B, The circum-papillary retinal nerve fiber layer thickness (RNFL) scan shows incorrect segmentation of the posterior border of the RNFL (white arrows), which leads to artifactually thick RNFL values (black arrows). C, The optical coherence tomography vertical line scan produced a vertical cup to disc ratio calculation of 1.0 at the reference plane 150  $\mu\text{m}$  above the retinal pigment epithelium. D, The neuroretinal rim Bruch's membrane opening-minimum rim width (blue arrows), which is the minimum distance between Bruch's membrane opening and the internal limiting membrane, was below normal limits.

limits in the OCT report. There was inferotemporal RNFL thinning that was coded as red. Inspection of the OCT image (Fig. 4B) revealed artifactual “thickening” of the temporal RNFL due to inaccurate segmentation of the posterior RNFL border. The cup to disc ratio calculated by the C++ code was 0.6 (Fig. 4C). Global neuroretinal rim MDB thickness was 298  $\mu\text{m}$ , and 3D reconstruction of the MDB neuroretinal rim showed focal inferior temporal neuroretinal rim thinning (Fig. 4D), which was consistent with the superior VF defect and inferior RNFL thinning.

**Case 4**

A 45-year-old Hispanic male was referred to our clinic for glaucoma evaluation. The patient had a history of a severe alkali burn and an elevated IOP of 50 mm Hg in his left eye. Six months before imaging, he had type I KPro and Ahmed glaucoma valve surgery. At the time of imaging, his BCVA was 20/30. His IOP was estimated to be between 15 and 18 mm Hg on 1 topical fixed-combination (brimonidine 0.2%/timolol maleate 0.5% tid). Examination of the optic disc

showed a cup to disc ratio of 0.6 with no focal notching of the neuroretinal rim. VF testing showed poor reliability (ie, 49% fixation loss) with generalized depression (MD was  $-11.92$  dB) and no localized scotomas (Figs. 5A, B). The circle scan images had a signal strength of 19 dB with segmentation artifacts of the posterior border of the RNFL and consequently, the reported global RNFL thickness value of 83  $\mu\text{m}$  was not reliable. Therefore, RNFL volume and retinal volume were computed for the CA1 annulus using the volume scans (Figs. 5C–F). Global RNFL volume in the annulus was 0.45  $\text{mm}^3$  and global retinal volume for CA1 was 1.55  $\text{mm}^3$ . Both RNFL volume and total retinal volume are consistent with values for normal patients from the spectral domain OCT in glaucoma prospective imaging database.<sup>27</sup>

**DISCUSSION**

The literature on KPro surgery has consistently reported a high incidence of glaucoma before KPro implantation, as well as new cases postoperatively.<sup>3–13</sup>

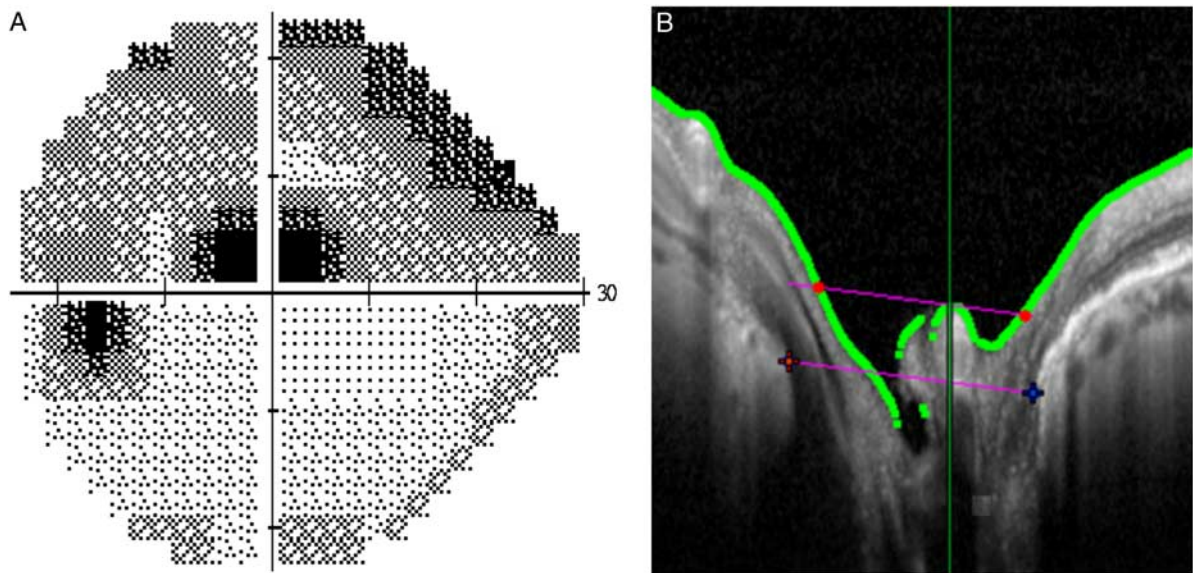


**FIGURE 3.** The clinical testing in a 56-year-old white woman who has a type I Boston Keratoprosthesis in her left eye for Stevens-Johnson syndrome. A, Visual field testing shows a superior paracentral defect. B, The optical coherence tomography vertical line scan through the optic nerve was processed with C++ code and calculated a vertical cup to disc ratio of 0.8 at a plane 150 μm above the retinal pigment epithelium.

Glaucoma in KPro patients can progress quickly and has been reported to be 7.5 times faster than progression in primary open angle glaucoma patients.<sup>1</sup> Therefore the diagnosis and close follow-up of this blinding disease in patients implanted with KPro is essential for timely treatment to maximum vision in these severely diseased and fragile eyes. Comprehensive imaging with OCT may enable better monitoring of glaucoma in these complex patients, in whom traditional testing is problematic.

The diagnosis and management of glaucoma in KPro patients is complex due to the difficulties in the ocular examination (ie, IOP measurements and cup to disc ratio assessments). As accurate Goldmann applanation tonometry is not possible in KPro patients, finger palpation is the most commonly employed method to grossly estimate IOP in KPro patients. Finger palpation has been demonstrated to be fairly accurate at detecting high levels of IOPs, particularly when performed by experienced observers.<sup>28–30</sup> However, the accuracy of finger palpation has never been validated in KPro patients. Because of the small diameter of the 3.0-mm polymethylmethacrylate KPro optic, clinical examination of the optic nerve is difficult (Fig. 4A). Furthermore, mydriasis is not possible in KPro patients but is critical for the reproducible cup to disc ratio estimates.<sup>31</sup>

Perimetry can be performed in KPro patients, and it remains an easily performed and reproducible method to diagnose and monitor glaucoma in this group of patients. This test remains a subjective tool, and the interpretation of this test depends on the reliability indices as well as the effects induced by the KPro optic itself. It has been demonstrated that the maximum visual angle seen through a KPro optic is between 90 and 95 degrees and that the KPro eye has a 50 degrees temporal VF compared with the normal temporal VF of around 90 degrees.<sup>32,33</sup> Therefore one should keep in mind the specific limitations of perimetry in the management of glaucoma in KPro patients. Case 4 illustrates the difficulties in interpreting VFs in KPro

patients. In addition to a high rate of fixation losses (7/15), the perimetric changes observed in this patient were suggestive of a general depression with an MD of  $-11.92$  dB and a PSD of 1.61 dB (Fig. 5, top). This illustrates the difficulty of getting reliable field tests in Kpro patients. Crnej et al<sup>1</sup> reported in their series that reliable VF was only present in 59% of KPro patients.

This series of cases illustrates that it is possible to obtain peripapillary 2D RNFL scans that are of good signal strength in KPro I and II eyes; however, 3 of the 4 cases showed RNFL segmentation errors, which render these scans unusable. It is important to attempt RNFL thickness measurements in KPro patients, because RNFL thickness is the most commonly used commercially available scan, and RNFL thinning is a strong indicator of glaucoma.<sup>15–17</sup> Plus, RNFL thinning or retinal ganglion cell death can occur before VF alterations<sup>34,35</sup> and may be a good metric for early diagnosis of glaucoma or detection of disease progression.<sup>35–37</sup> The high rate of segmentation errors in RNFL thickness measurements for KPro patients occurs for many possible reasons (Figs. 2B, 4B). For one, KPro patients usually present with advanced glaucoma, and progression often occurs quickly.<sup>1</sup> It is well known that accurate RNFL thickness measurements are more difficult to obtain in glaucoma patients with advanced disease because the glaucomatous disease causes both thinning of the RNFL and loss of RNFL reflectivity. When there is a decrease in RNFL reflectivity, it is more challenging for automated OCT algorithms to differentiate the posterior RNFL border from the less reflective underlying structures especially in patients with moderate and severe glaucoma.<sup>38</sup> Even in non-KPro patients, errors in RNFL thickness measurements have been reported to range from 18.0% to 46.7%.<sup>39–44</sup> Furthermore, the small size of the KPro optic may also limit the accuracy of 2D RNFL measurements. Smith et al<sup>45</sup> reported that acquisition of high-quality OCT images was not possible without pupillary dilation in about 25% of

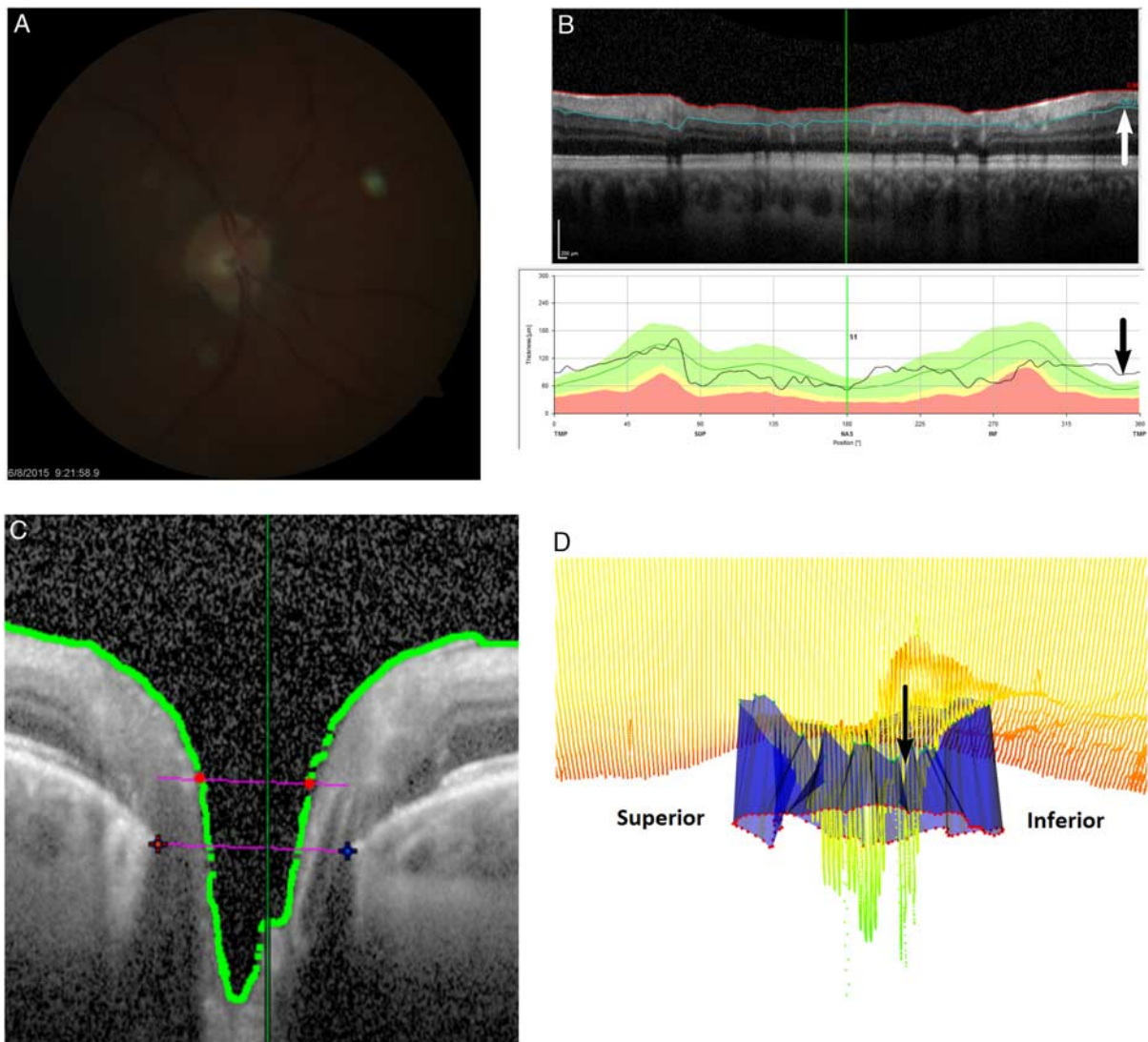


**FIGURE 4.** The clinical testing obtained in a 41-year-old white male who had a type I Boston Keratoprosthesis for severe alkali burn in his right eye. A, The cup to disc ratio was estimated to be 0.2 on the initial clinical assessment as shown on the fundus color photograph. B, The circumpapillary retinal nerve fiber layer (RNFL) scan shows incorrect segmentation of the posterior border of the RNFL (white arrows), which leads to artifactually thick RNFL values (black arrows). C, The optical coherence tomography (OCT) vertical line scan produced a vertical cup to disc ratio calculation of 0.6 at the reference plane 150  $\mu\text{m}$  above the retinal pigment epithelium (RPE). D, The 20 $\times$ 20 degrees OCT volume scan produced the 3-dimensional minimum distance band (MDB) shown in blue in this figure. The MDB is a circular band delimited by the shortest distance between the termination of the RPE (red dots) and the closest point on the cup surface (green dots). The MDB neuroretinal rim is shown in this figure and has focal inferotemporal thinning (black arrow).

patients, and that dilated scans were more reproducible and of higher quality than undilated scans. Even though RNFL thickness measurements are possible in KPro patients, this study shows that segmentation errors are common, and better OCT test parameters are needed in KPro patients.

In general, there is a poor agreement between the subjective cup to disc ratio determination on clinical examination and the objective measurements obtained using OCT. Both our study (cases 1 to 3) and the literature suggest that the cup to disc ratio by OCT is greater compared with clinical assessments.<sup>46,47</sup> The average difference between the clinically estimated cup to disc ratio and the OCT derived value in our patients was 0.3 (range, 0.1 to 0.5). Therefore, glaucoma diagnosis and follow-up in KPro patients should

not rely heavily on the cup to disc ratio, given its limitations and variability.

Cases 1, 2, and 4 are good examples where 3D derived diagnostic parameters (ie, the MDB neuroretinal rim parameter, the BMO-MRW neuroretinal rim parameter, 3D RNFL volume, and 3D retinal volume) have been used to overcome the limitations of 2D RNFL thickness values. Spectral domain OCT technology offers the possibility to acquire volume scans of the ONH with high speed and high resolution. Volume scans can then be used to process 3D volumetric structural parameters that have been shown to have superior diagnostic capability compared with traditional 2D RNFL thickness measurements.<sup>44,48,49</sup> Volume scans are denser than 2D RNFL scans and have the advantage of offering more sampling over a larger area. It is

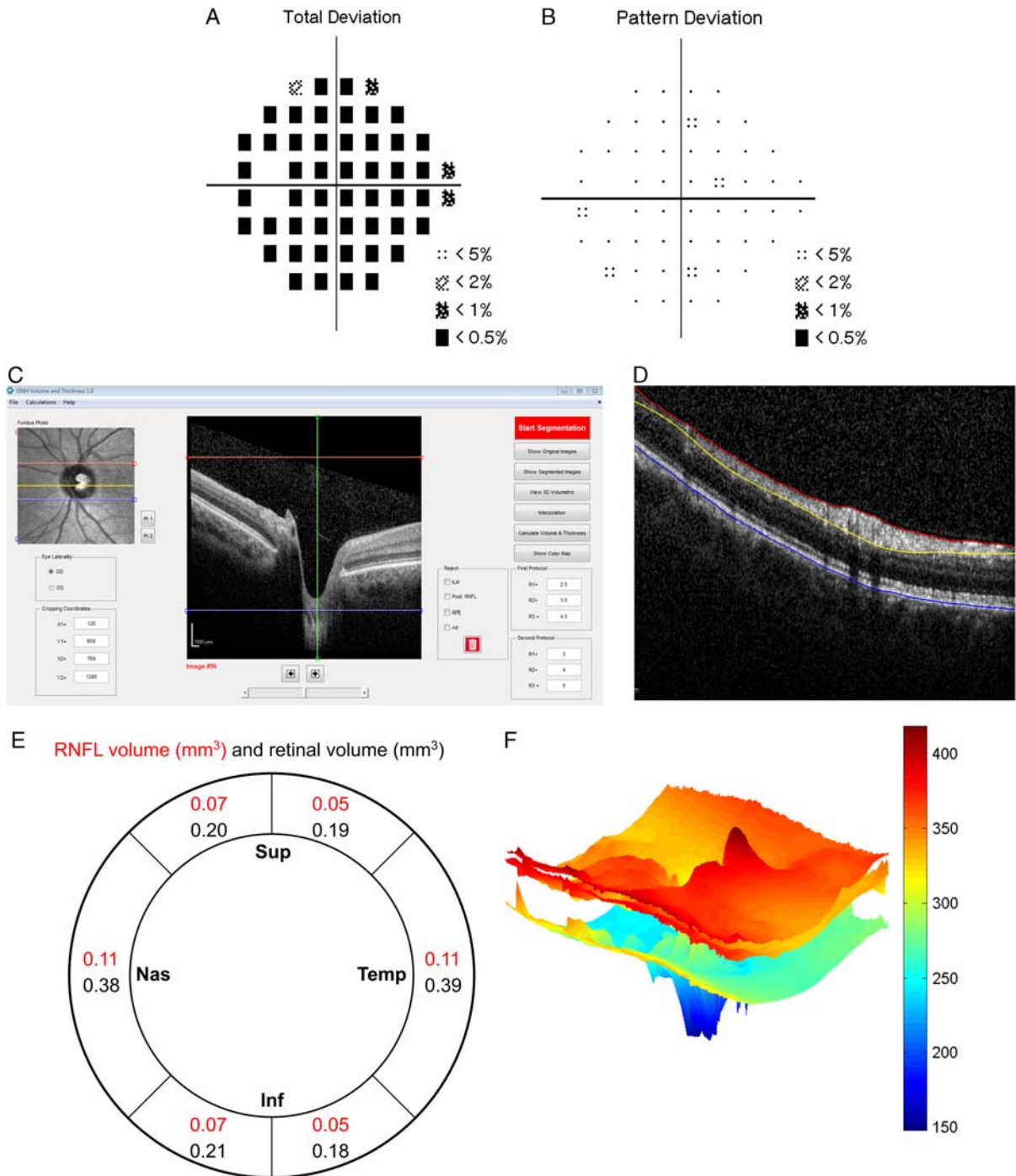


**FIGURE 5.** The clinical testing obtained in a 45-year-old Hispanic male who had type I Boston Keratoprosthesis for severe alkali burn in his left eye. A, The total deviation probability map of the 24-2 Humphrey visual field indicates generalized depression. B, The pattern deviation probability map of the 24-2 Humphrey visual field is within normal limits. C, The segmentation software interface was developed at the Massachusetts Eye and Ear Infirmary and was used to process the 3-dimensional (3D) volume scans of the optic nerve and peripapillary region. D, All 193 B-scans of the 3D volume set were automatically segmented using edge and intensity information, the 96th image of the 193 B-scan volume set is given as an example. The red line given by the algorithm corresponds to the internal limiting membrane (ILM), the yellow line delineates the posterior border of the retinal nerve fiber layer (RNFL) and the blue line delineates the retinal pigment epithelium (RPE). E, Using the information provided by the segmentation pattern the software calculates the RNFL volume in black as well as the retinal volume in red for each subdivision of the annulus located between 2 circles centered around the optic nerve. F, The software also gives a 3D map of the peripapillary area showing the plane of the RPE, ILM, and posterior border of the RNFL.

known that a larger sampling density provides better reproducibility.<sup>50,51</sup> Furthermore, recent papers from our team support the fact that 3D volume parameters (ie, 3D RNFL volume, 3D peripapillary retinal thickness and volume, and 3D neuroretinal rim thickness and volume) have the same or better diagnostic capability compared with peripapillary 2D RNFL thickness measurements.<sup>27,44,52,53</sup>

In conclusion, the diagnosis and management of glaucoma after KPro surgery should be considered a priority during postoperative follow-up visits. Clinical optic nerve examination, IOP assessment by finger palpation, disc photography, and VF testing have been classically used to evaluate KPro patients with glaucoma, but each of these methods has its limitations and can be supplemented by more objective and reproducible parameters derived from OCT optic nerve volume scans. Spectral domain OCT offers the possibility of evaluating KPro patients with 2D and 3D diagnostic parameters that are easily acquired in a clinic setting. Further large-scale studies are still needed to evaluate the diagnostic capability and reproducibility of OCT optic nerve volume scan in Kpro patients.

#### ACKNOWLEDGEMENTS

The authors would like to thank Kitiya Ratanawongphaibul, MD for her assistance and support with production of the figures.

#### REFERENCES

- Crnej A, Paschalis EI, Salvador-Culla B, et al. Glaucoma progression and role of glaucoma surgery in patients with Boston keratoprosthesis. *Cornea*. 2014;33:349–354.
- Lee R, Khoueir Z, Tsikata E, et al. Long-term visual outcomes and complications of Boston keratoprosthesis type II implantation. *Ophthalmology*. 2017;124:27–35.
- Netland PA, Terada H, Dohlman CH. Glaucoma associated with keratoprosthesis. *Ophthalmology*. 1998;105:751–757.
- Kamyar R, Weizer JS, de Paula FH, et al. Glaucoma associated with Boston type I keratoprosthesis. *Cornea*. 2012;31:134–139.
- Robert M-C, Pomerleau V, Harissi-Dagher M. Complications associated with Boston keratoprosthesis type I and glaucoma drainage devices. *Br J Ophthalmol*. 2013;97:573–577.
- Talajic JC, Agoumi Y, Gagné S, et al. Prevalence, progression, and impact of glaucoma on vision after Boston type I keratoprosthesis surgery. *Am J Ophthalmol*. 2012;153:267.e1–274.e1.
- Chew HF, Ayres BD, Hammersmith KM, et al. Boston keratoprosthesis outcomes and complications. *Cornea*. 2009;28:989–996.
- Aldave AJ, Kamal KM, Vo RC, et al. The Boston type I keratoprosthesis: improving outcomes and expanding indications. *Ophthalmology*. 2009;116:640–651.
- Bradley JC, Hernandez EG, Schwab IR, et al. Boston type I keratoprosthesis: the University of California Davis experience. *Cornea*. 2009;28:321–327.
- Aldave AJ, Sangwan VS, Basu S, et al. International results with the Boston type I keratoprosthesis. *Ophthalmology*. 2012;119:1530–1538.
- Patel AP, Wu EI, Ritterband DC, et al. Boston type I keratoprosthesis: the New York Eye and Ear experience. *Eye (Lond)*. 2012;26:418–425.
- Zerbe BL, Belin MW, Ciolino JB. Boston Type 1 Keratoprosthesis Study Group. Results from the multicenter Boston Type 1 Keratoprosthesis Study. *Ophthalmology*. 2006;113:1779.e1–1779.e7.
- Rivier D, Paula JS, Kim E, et al. Glaucoma and keratoprosthesis surgery: role of adjunctive cyclophotocoagulation. *J Glaucoma*. 2009;18:321–324.
- Banitt M. Evaluation and management of glaucoma after keratoprosthesis. *Curr Opin Ophthalmol*. 2011;22:133–136.
- Wu H, de Boer JF, Chen TC. Diagnostic capability of spectral-domain optical coherence tomography for glaucoma. *Am J Ophthalmol*. 2012;153:815.e2–826.e2.
- Schulze A, Lamparter J, Pfeiffer N, et al. Diagnostic ability of retinal ganglion cell complex, retinal nerve fiber layer, and optic nerve head measurements by Fourier-domain optical coherence tomography. *Graefes Arch Clin Exp Ophthalmol*. 2011;249:1039–1045.
- Na JH, Sung KR, Lee JR, et al. Detection of glaucomatous progression by spectral-domain optical coherence tomography. *Ophthalmology*. 2013;120:1388–1395.
- Chen TC, Hoguet A, Junk AK, et al. Spectral-domain OCT: helping the clinician diagnose glaucoma: a report by the American Academy of Ophthalmology. *Ophthalmology*. 2018;125:1817–1827.
- Qian CX, Hassanaly S, Harissi-Dagher M. Anterior segment optical coherence tomography in the long-term follow-up and detection of glaucoma in Boston type I Keratoprosthesis. *Ophthalmology*. 2015;122:317–325.
- Kang JJ, Allemann N, Cruz J de la, et al. Serial analysis of anterior chamber depth and angle status using anterior segment optical coherence tomography after Boston Keratoprosthesis. *Cornea*. 2013;32:1369–1374.
- Chen TC. Spectral domain optical coherence tomography in glaucoma: qualitative and quantitative analysis of the optic nerve head and retinal nerve fiber layer (an AOS thesis). *Trans Am Ophthalmol Soc*. 2009;107:254–281.
- Feuer WJ, Parrish RK, Schiffman JC, et al. The Ocular Hypertension Treatment Study: reproducibility of cup/disk ratio measurements over time at an optic disc reading center. *Am J Ophthalmol*. 2002;133:19–28.
- Zangwill L, Shakiba S, Caprioli J, Weinreb RN. Agreement between clinicians and a confocal scanning laser ophthalmoscope in estimating cup/disk ratios. *Am J Ophthalmol*. 1995;119:415–421.
- Kumar RS, Tan DTH, Por Y-M, et al. Glaucoma management in patients with osteo-odonto-keratoprosthesis (OOKP): the Singapore OOKP Study. *J Glaucoma*. 2009;18:354–360.
- Chauhan BC, O’Leary N, Almobarak FA, et al. Enhanced detection of open-angle glaucoma with an anatomically accurate optical coherence tomography-derived neuroretinal rim parameter. *Ophthalmology*. 2013;120:535–543.
- Mwanza J-C, Chang RT, Budenz DL, et al. Reproducibility of peripapillary retinal nerve fiber layer thickness and optic nerve head parameters measured with cirrus HD-OCT in glaucomatous eyes. *Invest Ophthalmol Vis Sci*. 2010;51:5724–5730.
- Khoeir Z, Jassim F, Poon LY-C, et al. Diagnostic capability of peripapillary three-dimensional retinal nerve fiber layer volume for glaucoma using optical coherence tomography volume scans. *Am J Ophthalmol*. 2017;182:180–193.
- Baum J, Chaturvedi N, Netland PA, et al. Assessment of intraocular pressure by palpation. *Am J Ophthalmol*. 1995;119:650–651.
- Birnbach CD, Leen MM. Digital palpation of intraocular pressure. *Ophthalmic Surg Lasers*. 1998;29:754–757.
- Rubinfeld RS, Cohen EJ, Laibson PR, et al. The accuracy of finger tension for estimating intraocular pressure after penetrating keratoplasty. *Ophthalmic Surg Lasers*. 1998;29:213–215.
- Kirwan JF, Gouws P, Linnell AET, et al. Pharmacological mydriasis and optic disc examination. *Br J Ophthalmol*. 2000;84:894–898.
- Sayegh RR, Avena Diaz L, Vargas-Martín F, et al. Optical functional properties of the Boston Keratoprosthesis. *Invest Ophthalmol Vis Sci*. 2010;51:857–863.
- Spector RH. Visual Fields. In: Walker HK, Hall WD, Hurst JW, eds. *Clinical Methods: The History, Physical, and Laboratory Examinations*, 3rd ed. Boston, MA: Butterworths; 1990.
- Quigley HA, Addicks EM, Green WR. Optic nerve damage in human glaucoma. III. Quantitative correlation of nerve fiber loss and visual field defect in glaucoma, ischemic neuropathy,



- papilledema, and toxic neuropathy. *Arch Ophthalmol*. 1982;100:135–146.
35. Kerrigan-Baumrind LA, Quigley HA, Pease ME, et al. Number of ganglion cells in glaucoma eyes compared with threshold visual field tests in the same persons. *Invest Ophthalmol Vis Sci*. 2000;41:741–748.
  36. Gordon MO, Kass MA. The Ocular Hypertension Treatment Study: design and baseline description of the participants. *Arch Ophthalmol*. 1999;117:573–583.
  37. Jaffe GJ, Caprioli J. Optical coherence tomography to detect and manage retinal disease and glaucoma. *Am J Ophthalmol*. 2004;137:156–169.
  38. Vanderschoot J, Vermeer KA, Boer JF de, et al. The effect of glaucoma on the optical attenuation coefficient of the retinal nerve fiber layer in spectral domain optical coherence tomography images. *Invest Ophthalmol Vis Sci*. 2012;53:2424–2430.
  39. Leal-Fonseca M, Rebolleda G, Oblanca N, et al. A comparison of false positives in retinal nerve fiber layer, optic nerve head and macular ganglion cell-inner plexiform layer from two spectral-domain optical coherence tomography devices. *Graefes Arch Clin Exp Ophthalmol*. 2013;252:321–330.
  40. Asrani S, Essaid L, Alder BD, et al. Artifacts in spectral-domain optical coherence tomography measurements in glaucoma. *JAMA Ophthalmol*. 2014;132:396–402.
  41. Moreno-Montañés J, Antón A, Olmo N, et al. Misalignments in the retinal nerve fiber layer evaluation using cirrus high-definition optical coherence tomography. *J Glaucoma*. 2011;20:559–565.
  42. Kim NR, Lim H, Kim JH, et al. Factors associated with false positives in retinal nerve fiber layer color codes from spectral-domain optical coherence tomography. *Ophthalmology*. 2011;118:1774–1781.
  43. Liu Y, Simavli H, Que CJ, et al. Patient characteristics associated with artifacts in spectralis optical coherence tomography imaging of the retinal nerve fiber layer in glaucoma. *Am J Ophthalmol*. 2015;159:565.e2–576.e2.
  44. Simavli H, Que CJ, Akduman M, et al. Diagnostic capability of peripapillary retinal thickness in glaucoma using 3D volume scans. *Am J Ophthalmol*. 2015;159:545.e2–556.e2.
  45. Smith M, Frost A, Graham CM, et al. Effect of pupillary dilatation on glaucoma assessments using optical coherence tomography. *Br J Ophthalmol*. 2007;91:1686–1690.
  46. Arnalich-Montiel F, Muñoz-Negrete FJ, Rebolleda G, et al. Cup-to-disc ratio: agreement between slit-lamp indirect ophthalmoscopic estimation and stratus optical coherence tomography measurement. *Eye*. 2006;21:1041–1049.
  47. Martinez-De-La-Casa JM, Saenz-Frances F, Fernandez-Vidal AM, et al. Agreement between slit lamp examination and optical coherence tomography in estimating cup-disc ratios. *Eur J Ophthalmol*. 2008;18:423–428.
  48. Shin JW, Uhm KB, Seong M, et al. Diffuse retinal nerve fiber layer defects identification and quantification in thickness maps. *Invest Ophthalmol Vis Sci*. 2014;55:3208–3218.
  49. Shin JW, Uhm KB, Seong M. Retinal nerve fiber layer defect volume deviation analysis using spectral domain optical coherence tomography. *Invest Ophthalmol Vis Sci*. 2014;56:21–28.
  50. Budenz DL, Chang RT, Huang X, et al. Reproducibility of retinal nerve fiber thickness measurements using the stratus OCT in normal and glaucomatous eyes. *Invest Ophthalmol Vis Sci*. 2005;46:2440–2443.
  51. Gurses-Ozden R, Ishikawa H, Hoh ST, et al. Increasing sampling density improves reproducibility of optical coherence tomography measurements. *J Glaucoma*. 1999;8:238–241.
  52. Simavli H, Poon LY-C, Que CJ, et al. Diagnostic capability of peripapillary retinal volume measurements in glaucoma. *J Glaucoma*. 2017;26:592–601.
  53. Tsikata E, Lee R, Shieh E, et al. Comprehensive Three-dimensional analysis of the neuroretinal rim in glaucoma Using high-density spectral-domain optical coherence tomography volume scans. *Invest Ophthalmol Vis Sci*. 2016;57:5498–5508.